ChemComm

RSC Publishing

COMMUNICATION

View Article Online
View Journal | View Issue

Cite this: *Chem. Commun.*, 2013, **49**, 4241

Received 15th October 2012,
Accepted 27th January 2013

DOI: 10.1039/c3cc40387d

www.rsc.org/chemcomm

Microwave synthesis of Au–Rh core–shell nanoparticles and implications of the shell thickness in hydrogenation catalysis†‡

Stephany García,[a] Rachel M. Anderson,[a] Hugo Celio,[b] Naween Dahal,[a] Andrei Dolocan,[b] Jiping Zhou[b] and Simon M. Humphrey*[a]

A microwave-assisted heating method allows for the convenient and reproducible synthesis of defined Au–Rh core–shell metallic nanoparticles with tuneable shell thicknesses. Nanoparticles with shells as thin as two Rh monolayers can be prepared, which are effective in vapour-phase hydrogenation catalysis at room temperature without the need for pre-treatment. Particles with Rh shells consisting of two or four Rh overlayers show similar catalytic properties and are both significantly more highly active than pure Rh nanoparticles, per mol of Rh employed.

Catalyst materials that contain highly dispersed, structurally-defined noble metal nanoparticles (NMNPs) are of timely interest in a wide range of heterogeneously-catalysed transformations.[1] The majority of critical industrial-scale reactions (oxidation, hydrogenation, cross-coupling, *etc.*) rely on expensive and often rare noble metals as the active catalytic species. NMNPs are very attractive alternatives to bulk metal catalysts, because their intrinsically high surface area to volume ratios results in a far greater proportion of surface atoms that can affect catalytic transformations.[2] They also offer potential for vastly superior, structure-related selectivity, based on intrinsic correlations between metal surface structure and catalytic reactivity.[1d,2]

Mixed-noble metal core–shell nanoparticles with defined surface structures are of particular current interest, because their catalytic properties are broadly tuneable based on the relative compositions of the two components.[3] Catalytic activity and selectivity of core–shell NMNPs can also be significantly enhanced *versus* pure metal NPs due to mixing of the electronic properties of each element at the core–shell interface, or due to atomic ensemble effects.[4] Moreover, core–shell NMNPs in which very thin shells (1–4 monolayers) of expensive and rare noble metals are supported around cores of less expensive and more abundant elements are industrially attractive. A number of recent novel synthetic studies using molecular precursors and organic 'capping agents' have shown promise in this regard.[5]

We have recently shown that microwave-assisted heating (MwH) can offer several key benefits in the solution-phase synthesis of small (3–12 nm) polymer-capped NMNPs of Rh, Pd or Pt.[6] Under otherwise identical reaction conditions, MwH was found to significantly improve overall NP size and shape, compared with conventional heating. Importantly, the catalytic hydrogenation reactivity of MwH-RhNPs was found to be significantly higher than for conventionally-prepared versions.[6] In this work, we have successfully extended the convenient and reproducible MwH method to the synthesis of Au–Rh core–shell hydrogenation catalysts, in which thin Rh shells were synthesised around AuNP seeds in a one-pot procedure. Au–Rh core–shell NPs have only been sparsely studied[7] and while some work for alloyed bimetallic NPs exist,[8] nothing appears to have been reported thus far concerning their catalytic properties. Au–RhNPs were targeted for the following reasons: (i) Au is stable towards oxidation, so well-defined AuNPs tend to be easily synthesized, and are highly stable once formed; (ii) both Au and Rh exhibit face-centred-cubic (FCC) lattices with only a slight lattice mismatch (4.08 *versus* 3.80 Å); (iii) Rh is highly active for hydrogenation, but Au is unable to dissociate H_2; and, (iv) there is an obvious economic motivation in limiting the quantity of Rh required per NP by using a majority of Au in the cores: according to the USGS, less than 30 t of Rh was mined per annum during the period 2006–2010;[9] during the same period, the cost of Rh peaked at \$210 g^{-1}, approximately seven times that of Au.

AuNPs were prepared by reducing $HAuCl_4{\cdot}H_2O$ with $NaBH_4$ in the presence of poly(vinylpyrrolidone) (PVP) in ethylene glycol at 150 °C for 30 min under MwH; borohydride was required because ethylene glycol alone cannot reduce Au(III) at 150 °C. The resulting isolated AuNPs were mostly spherical and near monodisperse, measuring 5.6 ± 1.5 nm, determined by transmission electron microscopy (TEM; Fig. 1A). The AuNPs were employed in the overgrowth step without further modification. Based on the desired thickness of the shell, a specific quantity of $RhCl_3{\cdot}xH_2O$ in ethylene glycol was added at a rate of 20.0 mL h^{-1} to the suspended AuNPs under MwH (controlled by syringe-pump). *In situ* reduction of Rh(III)

[a] *Department of Chemistry and Biochemistry, The University of Texas at Austin, 1 University Station A5300, Austin, TX 78712-0165, USA. E-mail: smh@cm.utexas.edu; Tel: +1 512-471-0312*

[b] *Texas Materials Institute, The University of Texas at Austin, 1 University Station C2201, Austin, TX 78712-0165, USA*

† This article is part of the *ChemComm* 'Emerging Investigators 2013' themed issue.

‡ Electronic supplementary information (ESI) available: XPS spectra, additional TOF-SIMS data, HRTEM images and EDS spectra for core–shell Rh–Au NPs, EXAFS spectra, TEM images and XPS data for the pre- and post-run catalyst materials, full experimental and catalysis details. See DOI: 10.1039/c3cc40387d

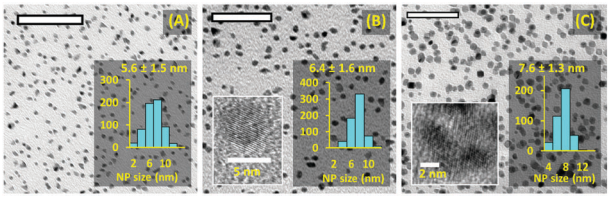

Fig. 1 TEM images, histograms and HRTEM images (inset) for: (A) AuNP cores; (B) thin-Rh; and, (C) thick-Rh core–shell NPs. Scale bars = 50 nm.

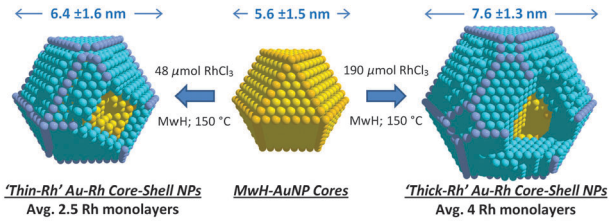

Scheme 1 Diagrammatical representation of the Au–Rh core–shell NPs structures, prepared using microwave-assisted synthesis: yellow/orange = Au; blue/violet = Rh.

by ethylene glycol facilitated the isotropic overgrowth of Rh(0) onto the AuNP seeds under MwH at 150 °C (Scheme 1). It should be noted that Rh has a significantly higher surface energy than Au (2.8 *versus* 1.6 J m^{-2}), so a hybrid structure in which Rh is deposited outside of an Au core is not the most thermodynamically-favoured arrangement.[8a] Also, Au(0) and Rh(0) are immiscible in the bulk, but alloying and/or core–shell inversion may still be possible on the nanoscale.[10]

The synthetic method employed here allows for simple modification of the Rh shell thickness over a broad range. In this initial report, the structural and catalytic properties of very thin and potentially strained Rh overlayers have been probed in detail, based on the assumption that increasingly thicker Rh shells should mimic the behaviour of bulk Rh. Specifically, 48 and 190 μmol of $RhCl_3$ was added to separate 3.0 mg batches of as-synthesized AuNPs. Initial analysis of the products by low and high-resolution transmission electron microscopy showed in both instances a majority of crystalline, spherical particles with a minority of more highly anisotropic structures. The Au–RhNPs had size distributions of 6.4 ± 1.6 nm and 7.3 ± 1.3 nm (denoted 'thin-Rh' and 'thick-Rh,' respectively; Fig. 1B and C; Fig. S1 and S2, ESI‡), which correspond to average particle size increases of 0.8 and 2.0 nm. These size increases approximate to 2.5 Rh monolayers (thin-Rh) and 4.0 Rh monolayers (thick-Rh), based on a metallic Rh–Rh layer-separation distance of 0.269 nm and assuming isotropic thickness of the Rh shells (Scheme 1).

To confirm that only Rh was present on the Rh–AuNP surfaces, samples from multiple preparations of the thin-Rh and thick-Rh samples were initially probed using X-ray Photoelectron Spectroscopy (XPS); the C1s signal at 285.1 eV (arising from the incorporated PVP polymer) was used as a reference. Additional control studies were run on the MwH-AuNP cores and 12.4 ± 2.1 nm MwH-RhNPs prepared using the same method (Fig. S3 and S4; Table S2, ESI‡).[6] The AuNPs displayed an intense peak for Au(0) (84.0 eV; $4f_{7/2}$) while the RhNPs gave a single peak which was assigned to Rh(I) (308.5 eV; $3d_{5/2}$). Interestingly, the thin-Rh core–shell NPs showed a marked decrease in intensity of the Rh signal at 308.5 eV, accompanied by the appearance of a second, new signal corresponding to Rh(0) (307.2 eV; $3d_{5/2}$), where Rh(0)/Rh(I) = 0.59 (Fig. S5 and Table S1, ESI‡). Thus, it appeared that the interaction of the Au core with the first 2–3 surface adlayers of Rh diminished the proportion of native oxidised Rh sites. As the amount of Rh adlayers increased for thick-Rh, the XPS spectra more closely resembled the appearance of the pure RhNPs, with a single signal at 308.3 eV for Rh(I) (Fig. S6, ESI‡). Meanwhile, the Au signal was extremely weak in thin-Rh samples (Rh/Au = 46) and was not observed for thick-RhNPs (Fig. S5 and S6, ESI‡), which indicated that Au was solely located in the core of the particles.§ A distinct Au(0) signal was only observed in both Rh-shell samples upon *in situ* Ar sputtering.

Comparison of the UV-vis absorption spectra for thin- and thick-Rh *versus* pure AuNPs and RhNPs prepared using the same MwH method also provided evidence for the deposition of Rh on to the Au cores (Fig. 2A). The plasmon peak at 540 nm for the AuNPs was quickly dampened as the Rh shell thickness increased. The original peak *ca.* 250 nm corresponding to the surface plasmon of the RhNPs was red shifted and became significantly more intense with increasing amount of added Rh, to resemble that of pure Rh. Powder X-ray diffraction analysis (PXRD) of the same core–shell structures showed reflections in the range 35–90° 2θ corresponding to pure Rh and Au (Fig. 2A, inset). The relative intensities of Au reflections were largely unchanged as a result of Rh overgrowth. However, Rh reflections were less intense and very broad for the thin-Rh samples, as should be expected for thin Rh overlayers; Rh reflections became slightly more defined as the Rh layer thickness was increased.

The Rh–Au core–shell structures were also analysed using time-of-flight secondary ion mass spectrometry (TOF-SIMS) to estimate the degree of surface separation between the two metals. Depth profiles for both Rh and Au were obtained from the secondary (ejected) ion counts as a function of sputtering time (Cs^+ ion beam at 500 eV, 63 nA sample current; Fig. 2B). For thin-Rh samples, the Rh/Au ratio was >1 for the first 30 seconds of sputtering and reached a maximum of ~8.5 after a few seconds. In comparison, the Rh/Au ratio for thick-Rh samples remained greater than parity for the first 350 seconds and reached a peak after 38 s, suggesting a thicker Rh shell (Fig. 2B; Fig. S7, ESI‡).

Line scan measurements and energy dispersive X-ray (EDS) analysis performed on thin Rh NPs (Fig. S8, ESI‡) showed both Rh and Au on single particles, the distribution of elements being consistent with an Au–Rh core–shell structure. In the case of thick-Rh NPs, no Au was observed (Fig. S9, ESI‡). However, area scans of several particle pockets did not display Au signals either

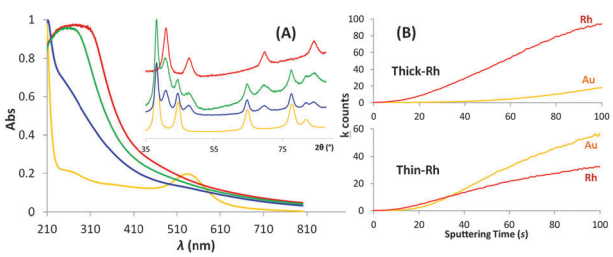

Fig. 2 (A) Comparisons of UV/vis spectra and PXRD (inset): yellow = 5.1 nm AuNP cores; blue = thin-Rh core–shell NPs; green = thick-Rh core–shell NPs; red = 12 nm RhNPs. (B) TOF-SIMS bulk Rh and Au *k*-counts during the first 100 s of sputtering with Cs^+.

which confirms that there were no isolated monometallic Au NPs or Rh core–Au shell particles.

In further support of the preparation of stable Rh–Au core–shell NPs, the core–shell NPs were probed by extended X-ray absorption fine structure (EXAFS) spectroscopy analysis (Fig. S10, ESI‡). Studies showed there was not a large contribution of Au–Rh or Rh–Au interactions in either the thin- or thick-Rh samples. This ruled out random alloying of the two metals and was also consistent with phase segregation. The Rh–Rh coordination number was found to be larger in the thick-Rh sample (7.9 ± 0.9) than in the thin-Rh sample (6.7 ± 0.8) (Table S3, ESI‡).

To assess the implications of NP structure upon the resulting surface catalytic properties, vapour-phase cyclohexene hydrogenation was used as a convenient model reaction. First, the Au, Rh and Rh–Au core–shell NPs were each supported on amorphous silica using a method reported previously (Fig. S11 and S12, ESI‡).[6] Next, milligram quantities of each catalyst material were studied using a single-pass reactor apparatus, in which a low pressure stream of H_2/He and cyclohexene were passed over the catalyst at 30 °C, with automated GC monitoring of the exhaust mixture. It is important to note that the catalysts were studied without any pre-treatment (see ESI‡ for full details). As expected, no turnover was observed for the supported AuNP cores because molecular hydrogen was not dissociatively chemisorbed by Au (Fig. 3, yellow line); meanwhile, the PVP-capped RhNPs showed steady-state activity after a short induction period (~4 min; Fig. 3, red line). Both the thin-Rh (Fig. 3, blue line) and thick-Rh (Fig. 3, green line) catalysts showed high activities for cyclohexene hydrogenation. This was expected, because the thin- and thick-Rh catalysts contain only 44 and 65 mol% Rh, respectively; TOFs were normalized per mol of Rh, assuming uniform cuboctahedral morphology. In contrast to the pure RhNPs, both core–shell catalysts were much slower to reach steady-state activity. The thick-Rh catalyst became stable after *ca.* 1 h on-stream, while the thin-Rh catalyst underwent a continual slow loss of activity up to 2 h. Presumably, the early catalytic instability observed for the core–shell species was due to adsorbate-induced surface restructuring of some initial higher-energy facets. The steady-state TOF values after 2 h on-stream were almost double that of the pure RhNPs. TEM analysis of the post-catalysis revealed that the NPs had retained their bulk morphology and had not become aggregated (Fig. S11–S14, ESI‡). This was not unexpected since the catalysts were not heated above 80 °C throughout the hydrogenation experiments. Secondly, XPS studies confirmed that the Rh(0)/Rh(I) ratio had increased significantly (thin-Rh = 5.0; thick-Rh = 2.5); meanwhile, there was still no detectable signal for Au, indicating that the core–shell structure was maintained during the catalysis (Fig. S15 and S16; Table S4, ESI‡).

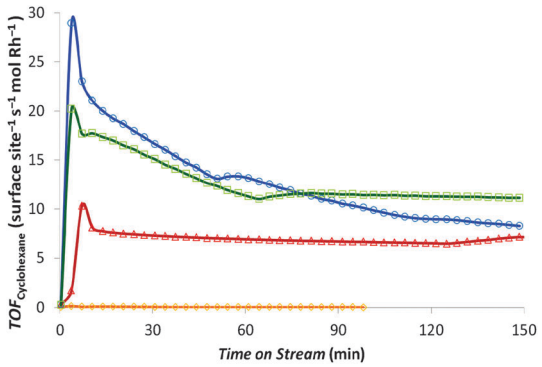

Fig. 3 Comparative catalysis data for cyclohexene hydrogenation: yellow = 5.1 nm AuNP cores; blue = thin-Rh core–shell NPs; green = thick-Rh core–shell NPs; red = 12.4 ± 2.1 nm MwH-RhNPs.

In summary, microwave-assisted synthesis is an effective method for the synthesis of Rh–Au core–shell NPs with tuneable shell dimensions. The resulting NPs can be employed directly in Rh-catalysed hydrogenation chemistry, with a significant increase in the relative proportion of catalytically-available surface Rh atoms compared to pure RhNPs.

The authors thank Dr Vincent M. Lynch and Dr Dwight Romanovicz for analytical assistance, Profs. Richard M. Crooks and Keith J. Stevenson for helpful discussions, The Welch Foundation (F-1738), The American Chemical Society Petroleum Research Fund (#51948-DNI3) and the Chemical Sciences, Geosciences, and Biosciences Division, Office of Basic Energy Sciences, Office of Science, U.S. Department of Energy (Contract: DE-FG02-09ER16090) for funding, and The National Science Foundation (0618242 and DMR-0923096) for the Kratos Axis Ultra XPS and ION-TOF TOF.SIMS 5 used in this work. Use of the NSLS is supported by the U.S. Department of Energy, Office of Science, Office of Basic Energy Sciences, under Contract No. DE-AC02-98CH10886. Beamline X18B at the NSLS is supported in part by the Synchrotron Catalysis Consortium, U.S. Department of Energy Grant No. DE-FG02-05ER15688.

Notes and references

§ The weak Au signal in the XPS spectrum of Au–Rh core–shell NPs does not indicate that the Rh layer is thicker than 10 nm; the particles have an overlayer of impurities and capping polymer of several nanometers that may prevent X-rays from penetrating the particle to the core.

1 (*a*) M. Haruta, *Gold Bull.*, 2004, **37**, 27; (*b*) G. J. Hutchings, *Chem. Commun.*, 2008, 1148; (*c*) L. N. Lewis, *Chem. Rev.*, 1993, **93**, 2693; (*d*) R. Narayanan and M. A. El-Sayed, *J. Phys. Chem. B*, 2005, **109**, 12663.
2 N. Semagina and L. Kiwi-Minsker, *Catal. Rev.*, 2009, **51**, 147.
3 (*a*) A. R. Kortan, R. Hull, R. L. Opila, M. G. Bawendi, M. L. Steigerwald, P. J. Carroll and L. E. Brus, *J. Am. Chem. Soc.*, 1990, **112**, 1327; (*b*) H. Lee, S. E. Habas, S. Kweskin, D. Butcher, G. A. Somorjai and P. Yang, *Angew. Chem., Int. Ed.*, 2006, **45**, 7824; (*c*) A. C. Dodd, *Powder Technol.*, 2009, **196**, 30; (*d*) R. G. Chaudhuri and S. Paria, *Chem. Rev.*, 2012, **112**, 2373.
4 (*a*) H. Kobayashi, M. Yamauchi, R. Ikeda and H. Kitagawa, *Chem. Commun.*, 2009, 4806; (*b*) S. Poulston, M. Tikhov and R. M. Lambert, *Catal. Lett.*, 1996, **42**, 167; (*c*) J. Storma, R. M. Lambert, M. Memmel, J. Onsgaard and E. Taglauer, *Surf. Sci.*, 1999, **436**, 259; (*d*) S. K. Beaumont, G. Kyriakou and R. M. Lambert, *J. Am. Chem. Soc.*, 2010, **132**, 12246; (*e*) D. A. Slanac, W. G. Hardin, K. P. Johnston and K. J. Stevenson, *J. Am. Chem. Soc.*, 2012, **134**, 9812.
5 (*a*) J. X. Wang, H. Inada, L. Wu, Y. Zhu, Y. Choi, P. Liu, W.-P. Zhou and R. R. Adzic, *J. Am. Chem. Soc.*, 2009, **131**, 17298; (*b*) S. Alayoglu and B. Eichhorn, *J. Am. Chem. Soc.*, 2008, **130**, 17479; (*c*) Y. Sun, B. Gates, B. Mayers and Y. Xia, *Nano Lett.*, 2002, **2**, 165; (*d*) C. J. DeSantis, A. C. Sue, M. M. Bower and S. E. Skrabalak, *ACS Nano*, 2012, **6**, 2617.
6 N. Dahal, S. Garcia, J. Zhou and S. M. Humphrey, *ACS Nano*, 2012, **6**, 9433.
7 (*a*) J. F. Li, J. R. Anema, Y.-C. Yu, Z.-L. Yang, Y.-F. Huang, X.-S. Zhou, B. Ren and Z.-Q. Tian, *Chem. Commun.*, 2011, **47**, 2023; (*b*) M. Tóth, J. Kiss, A. Oszkó and G. Pótári, *Top. Catal.*, 2012, **55**, 747; (*c*) N. Toshima, R. Ito, T. Matsushita and Y. Shiraishi, *Catal. Today*, 2007, **122**, 239.
8 (*a*) E. R. Essinger-Hileman, D. DeCicco, J. F. Bondi and R. E. Schaak, *J. Mater. Chem.*, 2011, **21**, 11599; (*b*) J. Kiss, A. Oszkó, G. Pótári and A. Erdóhelyi, *Vacuum*, 2012, **86**, 594; (*c*) J. Raskó and J. Kiss, *React. Kinet. Catal. Lett.*, 2007, **91**, 149; (*d*) A. Petér and J. K. A. Clarke, *J. Chem. Soc., Faraday Trans. 1*, 1976, **72**, 1201.
9 P. J. Loferski, US Geological Survey 2010 Minerals Yearbook.
10 E. I. Altman and R. J. Colton, *Surf. Sci. Lett.*, 1994, **304**, L400.